

Quantum trajectories for realistic measurement of a solid-state charge qubit

Neil P. Oxtoby,^{1,2,*} Prahlad Warszawski,³ Howard M. Wiseman,^{1,†} R. E. S. Polkinghorne,² and He-Bi Sun²

¹*Centre for Quantum Computer Technology, Centre for Quantum Dynamics,
School of Science, Griffith University, Nathan, QLD 4111, Australia*

²*Centre for Quantum Computer Technology, School of Physical Sciences,
The University of Queensland, St. Lucia, QLD 4072*

³*Centre for Quantum Dynamics, School of Science,
Griffith University, Nathan, QLD 4111, Australia*

(Dated: December 2, 2024)

We present a model for continuous DC-biased measurement of a coupled quantum dot (CQD) charge qubit by realistic measurement devices. Realistic measurement devices are modeled as ideal detectors embedded in an equivalent circuit for measurement. This adds noise to, and filters, the current through the detector. Our aim is to describe the evolution of the qubit state *conditioned* on the macroscopic output of the external circuit. We achieve this by generalizing a recently developed quantum trajectory theory for realistic photodetectors [P. Warszawski, H. M. Wiseman and H. Mabuchi, Phys. Rev. A **65** 023802 (2002)] to treat solid-state detectors. This yields stochastic equations whose (numerical) solutions are the “realistic quantum trajectories” of the conditioned qubit state. We apply our general theory to the following measurement devices: a DC single electron transistor (in two limits of operation) and a low transparency quantum point contact (tunnel junction limit). We discuss areas of application for our theory and its relation to previous work.

PACS numbers: 03.67.Lx, 73.23.-b, 73.23.Hk

I. INTRODUCTION

The field of research that surrounds the quest for a large-scale quantum computer is very exciting. At present, solid-state proposals^{1,2,3,4,5} seem promising. The ability to read out the state of the quantum bits (qubits) of information is of obvious importance in any quantum computational scheme. In this paper we consider continuous measurement of the state of a pair of coupled quantum dots (CQDs) occupied by a single excess electron. This constitutes a *charge* qubit. It is worth mentioning that spin qubits^{1,2,3,4,5} are considered more favourably for solid-state quantum computation due to their relatively long coherence times,⁶ but read-out may have to be performed via charge qubits using spin-to-charge conversion.^{1,7,8}

The conditional (or selective) evolution of a solid-state CQD qubit undergoing continuous measurement has been treated by a number of groups.^{9,10,11,12,13} The idealized qubit evolution in these papers is conditioned by the microscopic events occurring within the detector. Of these groups, only Ref. 13 (additional classical noise) and Ref. 12 (inefficiency) considered non-ideality of the detector. However neither considered the effect of a realistic measurement circuit, which we believe is a necessary step towards a satisfying theoretical description of this kind of continuous measurement. This is because real devices and circuits have noise and filtering properties that can be important. For clarity we use the terminology *detector* for an ideal detector and *measurement device* for a detector embedded within a measurement circuit. We derive a result equivalent to the non-ideal result of Ref. 13 in Appendix A using a stochastic master equation approach.

A *quantum trajectory*^{10,14,15,16} describes the Markovian stochastic evolution of an open quantum system conditioned on continuous monitoring of its output by an *ideal* detector. In an experiment the output from this detector is filtered through various noisy electronic devices. Due to the finite bandwidth of all electronic devices, there is a delay in the observer receiving the detector output signal. This implies that the evolution of the conditional state of the quantum system must be non-Markovian. A general method of describing this evolution was presented in recent papers^{17,18} by two of us in the context of photodetection, where it was applied to an avalanche photo-diode and a photo-receiver. In the present paper the general theory of Ref. 18 is applied to solid-state detectors. In our approach an equivalent circuit is used to model the realistic measurement. We also present example results for three specific detectors: 1. a single electron transistor operating in the DC mode (DC-SET), 2. a DC-SET with the island quantum dot adiabatically eliminated¹⁰ (hereafter ‘DC-SET A’) and 3. a low transparency quantum point contact (QPC) or tunnel junction.

We mention two factors to motivate realistic quantum trajectories. The first is that quantum trajectory theory has applications in the feedback control of continuously monitored open quantum systems.^{19,20,21,22,23,24,25,26} Before this can happen for realistic solid-state systems, the theory must be extended to incorporate uncertainties introduced by realistic detection. The second motivating factor is the emerging field of quantum computation, where the ability to relate realistically obtainable measurement results to the final qubit state is imperative for quantum error correction and state preparation.

The paper is organized as follows. We begin in the

next section by describing our models for the qubit and the three detectors (including the qubit's conditional dynamics in the ideal detector case). The equivalent circuit for realistic measurement is analyzed in Sec. III. The general method of deriving realistic quantum trajectories is presented in Sec. IV. In Sec. V we calculate equations that generate the realistic quantum trajectories for the three specific detectors mentioned. We discuss our results in Sec. VI and conclude in Sec. VII with a summary, comparison with previous work, and prospects for future work.

II. SYSTEM

In this section we describe the models for the qubit and the three detectors: 1. DC-SET, 2. DC-SET A and 3. low transparency QPC. Using a master equation formalism we present the conditional and ensemble average dynamics of the qubit state when measured by each ideal detector. The conditional dynamics in the ideal measurement case are represented by *stochastic* master equations, or quantum trajectories. We choose to present stochastic differential equations in the Itô formalism rather than the alternative Stratonovich formalism.²⁷ Extension of our theory to a realistic measurement case occurs later.

A. Qubit

Fig. 1 is a schematic representation of the CQD qubit and nearby detector. The CQDs are occupied by a single excess electron, the location of which determines the logical state of the qubit. We assume that each quantum dot has only one single-electron energy level available for occupation by the electron. These energy levels are denoted by E_n (*near* dot) and E_f (*far* dot). The electron tunnels between the two dots at the Rabi frequency Ω .

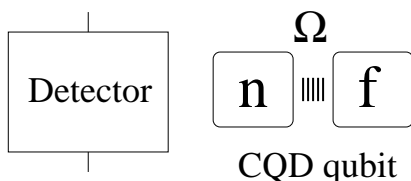


FIG. 1: Schematic of a coupled quantum dot charge qubit and solid-state detector.

Using the convention of $\hbar = 1$ (as we will for the entire paper), the total Hamiltonian for the qubit can be written as

$$\hat{H}_{qb} = E_n \hat{c}_n^\dagger \hat{c}_n + E_f \hat{c}_f^\dagger \hat{c}_f + \frac{\Omega_0}{2} (\hat{c}_n^\dagger \hat{c}_f + \hat{c}_f^\dagger \hat{c}_n), \quad (1)$$

where Ω_0 is the co-efficient of tunneling between the qubit dots (the Rabi frequency when $E_n = E_f$) and \hat{c}_n (\hat{c}_f) is the Fermi annihilation operator for the single available electron state within the *near* (*far*) CQD.

B. Dynamics of qubit undergoing ideal measurement

The state of a measured quantum system is affected by (i.e. conditioned by) the output of the detector via their mutual interaction. We describe the conditional dynamics of the measured qubit using a stochastic approach from a microscopic point of view. In the case of ideal measurement of a CQD qubit the state of the qubit is conditioned by electron tunneling events through the detector which constitute an ideal output current.

A number of formalisms exist that describe the evolution of a measured quantum system conditioned on a particular measurement result from the detector. The (ideal) conditional dynamics of continuously measured CQD systems have been treated by Bloch-type equations,⁹ quantum trajectory theory^{10,11,12} and a Bayesian formalism.^{13,25,28,29,30} The Bayesian formalism has been shown to practically co-incide with the quantum trajectory formalism with only notational differences (see the appendix of Ref. 11). All three formalisms coincide for the ensemble average dynamics of the measured CQD system. In this paper we describe the (Markovian) conditional dynamics of the qubit state with stochastic master equations. These are termed “quantum trajectories” because they track the state of the quantum system (CQDs) in time. Each of the quantum trajectories in this section describes the evolution of the qubit state *conditioned* on a particular realization of the tunneling events through the particular ideal detector. We also present the ensemble average master equations which are found by averaging over all possible quantum trajectories. In the Itô formalism this involves a simple substitution.

The following few subsections describe the microscopic models of each of the detectors considered and the dynamics of the qubit when monitored by each.

1. DC-SET

The mechanism that allows the position of the electron in the qubit to greatly influence the current through the SET is the so-called Coulomb blockade (for example see Ref. 31). Briefly, if the electrostatic energy of the island dot is minimized by having M (an integer) electrons on it, then the energy ‘cost’ of adding one electron to the island dot is $e^2/2C_\Sigma$, where C_Σ is the sum of all junction and gate capacitances in the SET and e is the electronic charge. This energy suppresses charge fluctuations (tunneling) at low temperatures ($k_B T < e^2/2C_\Sigma$) if the electrochemical potential in the leads is not sufficient to provide the extra electrostatic energy associated with the new electron configuration. It is said that the SET is ‘Coulomb blocked’ and very little current will flow.

If the SET is configured (via a change in gate voltage) so that the global electrostatic energy of the island dot is minimized by two different values of M , say M and $M + 1$, then electrons will be able to tunnel onto and

off the island dot one at a time without changing the global electrostatic energy. If there is a difference in the electrochemical potential of the leads, then the tunneling will be greater in one direction and a macroscopic current will flow through the external circuit. There are also higher order tunneling events such as co-tunneling that we do not present here as they may distract from the main results of this paper.

We assume that the SET is operated in a regime in which the leads cannot provide the charging energy to add electrons. Thus, the gate voltage controls whether current can flow or not. When used to measure a CQD qubit, the gate voltage is provided by the energy of the Coulomb interaction between the qubit electron and the island dot. When the qubit electron is in the near dot (labeled by n) the energy of the island dot is raised, changing the SET into a conducting state.

A diagram of the DC-SET is shown in Fig. 2. The island dot of the SET is separated from the leads by two tunnel junctions that are represented by capacitors C_1 and C_2 . The charges on these capacitors are denoted by Q_1 and Q_2 , respectively. Electron tunneling events through the junctions are represented by current sources. The average rates of tunneling through the junctions are denoted by r_j and r'_j ($j = 1, 2$), where a dash indicates that the SET is in a conducting state, i.e. $n = 1$ ($\hat{n} = \hat{c}_n^\dagger \hat{c}_n$). For simplicity we assume that electron tunneling through the detector occurs only in the direction shown by the arrows in Fig. 2. This is due to the bias voltage in the measurement circuit (see Sec. III) and is indicated by the ‘+’ and ‘-’ signs in Fig. 2. Due to the nature of the Coulomb blockade, we have

$$r'_1 \sim r'_2 \sim r_2 \gg r_1 . \quad (2)$$

The combined state of the qubit quantum dots and the SET quantum dot is described by the composite density matrix G . Although we consider the state of the SET island dot in a composite density matrix with the CQDs in the qubit, we assume that it is classical and that no superposition states exist within the SET. This will be true as long as the resistance of the tunnel junctions are greater than the resistance quantum $R_K \gtrsim h/e^2 \approx 26k\Omega$.³² The Hamiltonian for this system contains an additional term to those in the qubit Hamiltonian, Eq. (1), which accounts for the Coulomb blockade phenomenon. It is

$$\hat{H}_{CB} = \chi \hat{b}^\dagger \hat{b} \otimes \hat{c}_n^\dagger \hat{c}_n , \quad (3)$$

where b is the Fermi annihilation operator for the SET island dot and χ is the additional energy of an excess electron on the island dot when the near CQD is occupied. Thus, the total Hamiltonian for the composite qubit-plus-island-dot system is

$$\hat{H}_{SET} = \hat{I} \otimes \hat{H}_{qb} + \hat{H}_{CB} , \quad (4)$$

where \hat{I} is the 2×2 identity matrix.

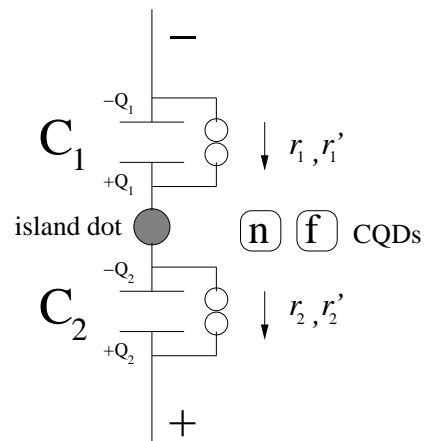


FIG. 2: An equivalent circuit for a DC biased single electron transistor (DC-SET). The direction of electron tunneling is indicated by the arrows. In the limit of an adiabatically eliminated island dot (‘DC-SET A’), the second tunnel junction is effectively removed so that electrons tunnel out of the island dot immediately upon tunneling into it through junction 1.

A realistic observer cannot tell when a tunneling event into, or out of, the SET dot occurs. However, we argue that in principle this information would be contained in the movement of the Fermi sea electrons in the leads attached to the SET. Thus, we can legitimately represent the *conditional* evolution of $G(t)$ (denoted with a superscript μ) in terms of these microscopic events. We treat tunneling events that are different due to the different qubit state as being classically indistinguishable. That is, an electron tunneling out of the SET when the nearer qubit dot is occupied ($n = 1$) is not practically distinguishable from an electron that tunnels out when the further dot is occupied. In principle even these electrons could be distinguished as the altered potential of the SET will cause differing amounts of energy to be dissipated into the Fermi sea. It is not important to consider this because both types of electrons will lead to the same amount of current flowing in the external circuit. The conditional evolution of $G(t)$ is given by the following stochastic master equation

$$\begin{aligned} dG^\mu(t) = & dN_1(t) \left\{ \frac{\mathcal{S}_1}{\text{Tr}[\mathcal{S}_1 G^\mu(t)]} - 1 \right\} G^\mu(t) \\ & + dN_2(t) \left\{ \frac{\mathcal{S}_2}{\text{Tr}[\mathcal{S}_2 G^\mu(t)]} - 1 \right\} G^\mu(t) \\ & - dt \mathcal{H} \left[\frac{1}{2} \hat{R} + i \hat{H}_{SET} \right] G^\mu(t) . \end{aligned} \quad (5)$$

The operator \hat{R} and superoperators \mathcal{S}_1 and \mathcal{S}_2 are defined

as follows

$$\hat{R} = r'_1 \hat{b} \hat{b}^\dagger \otimes \hat{n} + r_1 \hat{b} \hat{b}^\dagger \otimes (1 - \hat{n}) \\ + r'_2 \hat{b}^\dagger \hat{b} \otimes \hat{n} + r_2 \hat{b}^\dagger \hat{b} \otimes (1 - \hat{n}) , \quad (6)$$

$$\mathcal{S}_1 = r'_1 \mathcal{J} [\hat{b}^\dagger \otimes \hat{n}] + r_1 \mathcal{J} [\hat{b}^\dagger \otimes (1 - \hat{n})] , \quad (7)$$

$$\mathcal{S}_2 = r'_2 \mathcal{J} [\hat{b} \otimes \hat{n}] + r_2 \mathcal{J} [\hat{b} \otimes (1 - \hat{n})] . \quad (8)$$

We have also introduced the classical point processes $dN_1(t)$ and $dN_2(t)$. They represent the number (either 0 or 1) of electron tunneling events through the first and second SET junctions in an infinitesimal time interval $[t, t + dt)$, respectively. For an operator argument \hat{X} , the superoperators \mathcal{H} and \mathcal{J} are defined by

$$\mathcal{H} [\hat{X}] G = \hat{X} G + G \hat{X}^\dagger - \text{Tr} \left[(\hat{X} + \hat{X}^\dagger) G \right] G , \quad (9)$$

$$\mathcal{J} [\hat{X}] G = \hat{X} G \hat{X}^\dagger . \quad (10)$$

As intended, the event corresponding to an electron tunneling onto the SET dot is represented by an incoherent mixture of the two possible paths by which this can occur; this is the first term of the conditional master equation (5). Tunneling off the SET dot is treated similarly (in the second term). The final term in Eq. (5) represents the evolution of $G^\mu(t)$ that is due to the Hamiltonian and the null measurement of no SET tunneling events.

The ensemble average evolution of $G(t)$ is found by averaging over all possible trajectories given by Eq. (5). In the Itô formalism, this simply involves substituting the expectation values of the stochastic increments dN_1 and dN_2 into Eq. (5). These expectation values represent the average tunneling rates through each junction and can be expressed as the following operator expressions

$$\text{E} [dN_1(t)] = dt \text{Tr} [\mathcal{S}_1 G^\mu(t)] , \quad (11a)$$

$$\text{E} [dN_2(t)] = dt \text{Tr} [\mathcal{S}_2 G^\mu(t)] . \quad (11b)$$

We use a Roman font E to denote a classical expectation value. Omitting time arguments for simplicity, substitution of these equations into the quantum trajectory (5) yields the following ensemble average (unconditional) master equation for G

$$\dot{G} = -i [\hat{H}_{SET}, G] + r'_1 \mathcal{D} [\hat{b}^\dagger \otimes \hat{n}] G + r'_2 \mathcal{D} [\hat{b} \otimes \hat{n}] G \\ + r_1 \mathcal{D} [\hat{b}^\dagger \otimes (1 - \hat{n})] G + r_2 \mathcal{D} [\hat{b} \otimes (1 - \hat{n})] G \\ \equiv \mathcal{L}_1 G . \quad (12)$$

A similar master equation is considered for a superconducting SET measuring the state of a Cooper-pair box in Ref. 33. The Lindblad superoperator \mathcal{D} represents the irreversible part of the system evolution — the decoherence. \mathcal{D} is defined in terms of two other superoperators, \mathcal{J} and \mathcal{A} :

$$\mathcal{D} [\hat{X}] G \equiv \mathcal{J} [\hat{X}] G - \mathcal{A} [\hat{X}] G , \quad (13)$$

where the jump superoperator \mathcal{J} is defined by Eq. (10) and the anti-commutating superoperator is defined by

$$\mathcal{A} [\hat{X}] G \equiv \frac{1}{2} (\hat{X}^\dagger \hat{X} G + G \hat{X}^\dagger \hat{X}) . \quad (14)$$

These superoperators, introduced in Ref. 15, are used commonly in the field of quantum optics measurement theory. The ease of the averaging process when using the Itô formalism highlights a considerable advantage that it has over the Stratonovich formalism.

The state matrix for the qubit is found by tracing over the SET island dot: $\rho = \text{Tr}_{SET} [G]$.

2. DC-SET A

We can simplify the SET model greatly by adiabatically eliminating the SET island dot. We assume that $r'_2, r_2 \gg \Omega, r'_1, r_1$. This means that once an electron tunnels onto the island, it immediately tunnels off, effectively removing the second junction. We wish to continue to have the Coulomb blockade mechanism in place, so we require $\chi \gg r_2$. This model was introduced in Ref. 10. It allows consideration of the qubit state matrix alone, rather than the combined qubit-plus-island-dot state matrix.

The stochastic evolution of the qubit state when the qubit is measured by the DC-SET A is described by¹⁰

$$d\rho^\mu(t) = dN(t) \left\{ \frac{\lambda_0 + \lambda_1 \mathcal{J} [\hat{n}] + 2\lambda_0 \mathcal{D} [\hat{n}]}{\text{E}[dN(t)]/dt} - 1 \right\} \rho^\mu(t) \\ + dt \left\{ -\lambda_1 \mathcal{A} [\hat{n}] \rho^\mu(t) + \lambda_1 \text{Tr} [\rho^\mu(t) \hat{n}] \rho^\mu(t) \right. \\ \left. - i[\hat{H}_{qb}, \rho^\mu(t)] \right\} . \quad (15)$$

In this case, the expectation value of $dN(t)$ is given by

$$\text{E}[dN(t)] = dt \text{Tr} [(\lambda_0 + \lambda_1 \mathcal{J} [\hat{n}] + 2\lambda_0 \mathcal{D} [\hat{n}]) \rho^\mu(t)] \\ = dt \{ \lambda_0 + \lambda_1 \text{Tr} [\rho^\mu(t) \hat{n}] \} . \quad (16)$$

Averaging over the stochastic point process $dN(t)$ in a similar fashion to the previous section yields the following Markovian unconditional master equation for the qubit state matrix

$$\frac{d\rho}{dt} = -i[\hat{H}_{qb}, \rho] + \gamma \mathcal{D} [\hat{n}] \rho \equiv \mathcal{L}_2 \rho , \quad (17)$$

where the decoherence rate is given by

$$\gamma = 2\lambda_0 + \lambda_1 . \quad (18)$$

Here $\lambda_0 = r_1$ is the (effective) rate of tunneling through the DC-SET A when the island dot is Coulomb blocked (the quiescent rate) and $\lambda_1 = r'_1 - r_1$ is the additional rate of tunneling through the detector when the Coulomb blockade is lifted, i.e. when $n = 1$.

3. Low transparency QPC

A diagram of a low transparency QPC (or tunnel junction) is shown in Fig. 3. Again we represent the tunnel junction by a capacitance C_1 and electron tunneling events through the junction by a current source. The charge on the junction capacitor is denoted Q_1 . The average quiescent rate of tunneling through the QPC is λ_0 which we assume occurs when the CQD electron is in the near dot due to electrostatic repulsion. The additional rate λ_1 occurs when the far CQD is occupied. The QPC theory presented below reflects these choices. However, if the situation is the opposite and the maximum tunneling rate through the QPC occurs when the near CQD is occupied, the theory can be easily modified to reflect this. We choose this model for the purpose of comparison with other work.^{9,11,25,28,29,30,34}

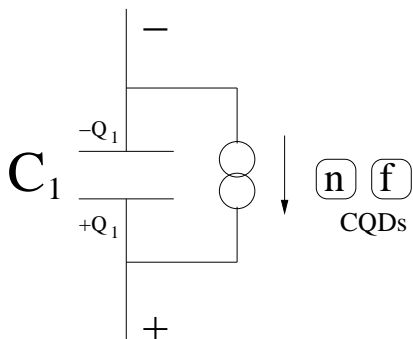


FIG. 3: An equivalent circuit for a low transparency QPC or tunnel junction. The arrow indicates the direction of electron tunneling through the QPC.

For the low transparency QPC we have based our ideal measurement model on that of Ref. 11. The quantum jump behaviour of electrons through the QPC causes the evolution of the qubit state to be described by the following Itô stochastic master equation

$$d\rho^\mu(t) = dN(t) \left\{ \frac{\mathcal{J}[\mathcal{T} + \mathcal{X}\hat{n}]}{\mathbb{E}[dN(t)]/dt} - 1 \right\} \rho^\mu(t) + dt \left\{ -\mathcal{A}[\mathcal{T} + \mathcal{X}\hat{n}] \rho^\mu(t) + \frac{\mathbb{E}[dN(t)]}{dt} \rho^\mu(t) - i[\hat{H}_{qb}, \rho^\mu(t)] \right\}, \quad (19)$$

where the expectation value of $dN(t)$ is

$$\begin{aligned} \mathbb{E}[dN(t)] &= dt \text{Tr}[\mathcal{J}[\mathcal{T} + \mathcal{X}\hat{n}] \rho^\mu(t)] \\ &= dt \{ \lambda_0 + \lambda_1 \text{Tr}[(1 - \hat{n})\rho^\mu(t)] \}. \end{aligned} \quad (20)$$

Again, the ensemble average dynamics are found by taking the expectation value of Eq. (19). The result is the following unconditional master equation for the qubit state matrix when measured by a low transparency QPC

$$\frac{d\rho}{dt} = -i[\hat{H}_{qb}, \rho(t)] + \mathcal{D}[\mathcal{T} + \mathcal{X}\hat{n}] \rho(t) \equiv \mathcal{L}_3 \rho. \quad (21)$$

For simplicity we have assumed real tunneling amplitudes whereby

$$\mathcal{T} = \sqrt{\lambda_0 + \lambda_1} \quad \text{and} \quad (22a)$$

$$\mathcal{X} = \sqrt{\lambda_0 - \mathcal{T}}. \quad (22b)$$

In the model of Ref. 11, Complex tunneling amplitudes are allowed for in the model of Ref. 11 and the generalization here is straight-forward.

We can simplify the presentation of the QPC and DC-SET A equations by writing the stochastic master equations (15) and (19) in the following concise form:

$$d\rho^\mu(t) = dN(t) \left\{ \frac{\mathcal{S}}{\text{Tr}[\mathcal{S}\rho^\mu(t)]} - 1 \right\} \rho^\mu(t) - dt \mathcal{H} \left[\frac{1}{2} \hat{R} + i\hat{H}_{qb} \right] \rho^\mu(t), \quad (23)$$

where the *device-specific* operator \hat{R} and superoperator \mathcal{S} are defined for the DC-SET A to be

$$\hat{R} \equiv \lambda_1 \hat{n}, \quad (24a)$$

$$\mathcal{S} \equiv \lambda_0 + \lambda_1 \mathcal{J}[\hat{n}] + 2\lambda_0 \mathcal{D}[\hat{n}], \quad (24b)$$

and for the low transparency QPC to be

$$\hat{R} \equiv (\mathcal{T} + \mathcal{X}\hat{n})^2, \quad (25a)$$

$$\mathcal{S} \equiv \mathcal{J}[\mathcal{T} + \mathcal{X}\hat{n}]. \quad (25b)$$

Note the similarities between the form of the combined DC-SET A/QPC ideal quantum trajectory (23) and that of the DC-SET (5). It is easy to see that Eq. (23) is a special case of Eq. (5). Thus, for the work in the following sections we derive equations for the DC-SET from which the equations for the other two detectors can be obtained.

III. EQUIVALENT CIRCUIT FOR REALISTIC MEASUREMENT

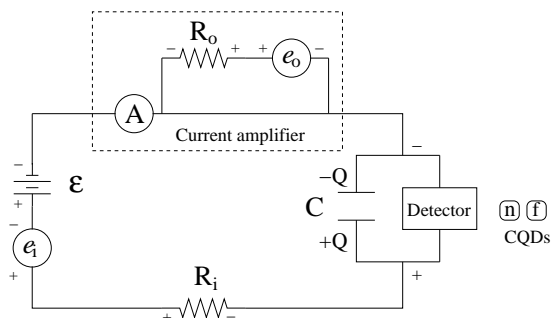


FIG. 4: A schematic of our equivalent circuit for realistic measurement of the state of a CQD charge qubit. The circuit can be considered as consisting of three parts at three temperatures: detector ($T \sim mK$), current amplifier ($T_o \sim 4K$) and miscellaneous circuit components (room temperature T_i).

Our equivalent circuit for realistic measurement of the CQDs is shown in Fig. 4. The circuit is biased by a non-ideal DC voltage consisting of an ideal voltage ε and a noisy voltage source e_i . This (white) noise source includes the Johnson-Nyquist noise from the equivalent circuit resistance R_i . The small current through the detector is amplified, then measured. A realistic observer will see white noise in addition to the current through the detector. This is modeled as an additional output (noise) current e_o/R_o and an ideal ammeter. Any filtering that may occur due to capacitance within the amplifier is considered to be significantly less than that due to the parasitic capacitance C and is ignored. It is important to note that the circuit components are not necessarily representative of an actual experimental setup. For example, an amplifier does not consist of a noisy voltage and a resistor, rather the observed effect of amplification of the current through the SET is the addition of an output noise e_o/R_o to the observed current. As such, each resistor is assigned an *effective* temperature: the circuit is at laboratory temperature T_i , the detector-CQD system is at cryogenic temperature $T \sim mK$ and the amplifier is at temperature $T_o \sim 4K$.

The *parasitic* capacitance C across the detector is due to the large cross-sectional area of the leads relative to the detector junctions.

The specific detector examples can be analyzed by substituting the appropriate detector circuit into the measurement circuit of Fig. 4. We analyze the equivalent circuit with the DC-SET as detector and produce expressions for the measured current $\mathcal{I}(t)$ and the evolution of the parasitic capacitor charge $Q(t)$. The variable $Q(t)$ is used to describe the state of the classical system — the realistic measurement device (detector plus circuit).

A. No tunneling through SET

Analysis of the measurement circuit (with the DC-SET as detector) using Kirchhoff's electrical circuit laws and assuming no electron tunneling events through the SET yields the following Itô differential equation for the increment in Q due to the circuit components

$$dQ(t) = \frac{1}{F} \left(-\frac{Q(t)}{R_i C} + \frac{\varepsilon}{R_i} + \frac{e_i}{R_i} \right) dt, \quad (26)$$

where F is a dimensionless quantity given by

$$F = 1 + \frac{C_1 C_2}{C(C_1 + C_2)}. \quad (27)$$

These equations are valid for the DC-SET A and QPC with the substitution $C_2 = 0$.

Similar analysis yields an expression for the measured current as a function of time, valid for all the detectors:

$$\mathcal{I}(t) = -\frac{Q(t)}{R_i C} + \frac{\varepsilon}{R_i} + \frac{e_i}{R_i} + \frac{e_o}{R_o}. \quad (28)$$

For the purposes of our work it is useful to express the (Johnson-Nyquist) noise sources e_i and e_o in terms of stochastic increments. In the steady state Johnson-Nyquist voltage noise is *white* noise and has a flat spectrum

$$S = 2k_B T R, \quad (29)$$

where T is the temperature of the noise source with resistance R and k_B is Boltzmann's constant. The current spectrum ('spectral density') definition³⁵ used here is⁴⁸

$$S(\omega) = \int_{-\infty}^{\infty} \exp[i\omega\tau] G(\tau) d\tau, \quad (30)$$

where $G(\tau)$ is the two-time autocorrelation function of the measured current. Obviously a current flow is not an equilibrium situation, but for reasonable bias voltages the approximation of Eq. (29) remains valid.³⁶ For simplicity, we take the flat spectra of the input and output voltage noises to be $2D_i R_i^2$ and $2D_o R_o^2$, respectively. This allows us to write Eq. (26) and Eq. (28) in terms of the input and output Wiener processes, $dW_i(t)$ and $dW_o(t)$, as

$$dQ(t) = \frac{1}{F} \left[\left(-\frac{Q(t)}{R_i C} + \frac{\varepsilon}{R_i} \right) dt + \sqrt{D_i} dW_i(t) \right], \quad (31)$$

$$\mathcal{I}(t) = -\frac{Q(t)}{R_i C} + \frac{\varepsilon}{R_i} + \sqrt{D_i} \frac{dW_i(t)}{dt} + \sqrt{D_o} \frac{dW_o(t)}{dt}, \quad (32)$$

where $D_i = 2k_B T_i / R_i$ and $D_o = 2k_B T_o / R_o$. These expressions correct the expressions in Refs. 17 and 18 from $4k_B T / R$ to $2k_B T / R$. The Wiener increment is related to Gaussian white noise $\xi(t)$ by $dW(t) = \xi(t)dt$. Gaussian white noise has statistics of²⁷

$$E[\xi(t)] = 0, \quad (33a)$$

$$E[\xi(t)\xi(t')] = \delta(t - t'). \quad (33b)$$

B. Tunneling events

We now consider the jump in charge on the parasitic capacitor due to electron tunneling events through both junctions of the SET. Again we present a general derivation for the DC-SET from which the (simpler) results for the DC-SET A and QPC can be obtained. We consider the charge on the capacitors C_1 and C_2 , i.e. $\pm Q_1$ and $\pm Q_2$, and analyze the changes in these values due to electron tunneling events onto and off the SET island dot.

Consider first tunneling onto the island dot. We use a prime to denote immediately after a tunneling event. If the Coulomb interaction between the SET island dot and the qubit is such that the charging energy of placing electrons on the island dot restricts the charge on it to M and $M + 1$ excess electrons, the following relationships

hold after a tunneling event *onto* the SET island dot

$$-Q' - Q'_1 = -Q - Q_1 - e, \quad (34a)$$

$$Q'_1 - Q'_2 = (M + 1)e, \quad (34b)$$

$$Q' + Q'_2 = Q + Q_2, \quad (34c)$$

$$\frac{Q}{C} = \frac{Q_1}{C_1} + \frac{Q_2}{C_2}, \quad (34d)$$

where $e = -|e|$ is the charge on an electron. Using these relationships along with the before-jump relationships (which are simple to derive) yields the jump in the charge on the parasitic capacitor due to an electron tunneling onto the SET island dot:

$$Q' - Q = \frac{e}{F} \frac{C_2}{C_1 + C_2} \equiv e_1. \quad (35)$$

With the prime now indicating immediately after a tunneling *off* event, the following relationships hold after a tunneling event *off* the SET island dot:

$$-Q' - Q'_1 = -Q - Q_1, \quad (36a)$$

$$Q'_1 - Q'_2 = Me, \quad (36b)$$

$$Q' + Q'_2 = Q + Q_2 + e \quad (36c)$$

and the voltage relationship, Eq. (34d), is still valid. We then have the jump in the parasitic capacitor charge due to a tunneling off event:

$$Q' - Q = \frac{e}{F} \frac{C_1}{C_1 + C_2} \equiv e_2. \quad (37)$$

Adding these results to Eq. (31) produces the following Itô differential equation for the change in the charge on the parasitic capacitor when the detector is a DC-SET:

$$dQ(t) = \frac{1}{F} \left\{ [-\alpha Q(t) + \beta] dt + \sqrt{D_i} dW_i(t) \right\} + e_1 dN_1(t) + e_2 dN_2(t), \quad (38)$$

where $dN_{1,2}(t)$ are the stochastic point processes introduced in Sec. IIB that are used to represent tunneling events through junctions 1 and 2. We have introduced the simplifying notations $\alpha = 1/R_i C$ and $\beta = \varepsilon/R_i$. The solution to this differential equation gives the value of $Q(t)$ that may be substituted into Eq. (32) to give a lengthy expression for the measured current.³⁷

For the other detectors ($C_2 = 0$) there is only one tunneling process $dN(t)$. Substitution of $C_2 = 0$ removes $dN_1(t)$ and leaves $dN_2(t)$. This can seem counter-intuitive since $C_2 = 0$. However, the increment $dN_2(t)$ represents the process that contributes directly to the measured current in the circuit external to the DC-SET — as the increment $dN(t)$ does in the case of the other two detectors. Thus, $dN_2(t) = dN(t)$ for the DC-SET A and QPC.

IV. DERIVATION OF REALISTIC QUANTUM TRAJECTORIES

The derivation of realistic quantum trajectories follows a number of well defined steps as presented for photodetectors in Ref. 18. In this section we present a general derivation of realistic quantum trajectories for solid-state detectors appropriate to our measurement circuit. We begin by summarizing the procedure.

The evolution of the state of the measurement device $Q(t)$ is represented by an Itô stochastic differential equation. A realistic observer will not be able to track $Q(t)$ due to the randomness of the microscopic events occurring within the device. We therefore find an equation that tracks the *probability* of the various states of the measurement device being occupied. This is called a stochastic differential Chapman-Kolmogorov equation (SDCKE). It is a generalization of the deterministic differential Chapman-Kolmogorov equation discussed in Ref. 27. The SDCKE incorporates the (unobservable) microscopic stochastic events occurring within the SET. Some of these noise processes are the stochastic jumps that also occur in the stochastic master equation (5).

Based on the realistic measurement result \mathcal{I} and the prior probability distribution for the state of the measurement device, the best estimate of the updated state is found. This is achieved using Bayesian analysis.³⁸ The resulting equation for the probability distribution is called a Kushner-Stratonovich equation (KSE) in the case of Gaussian white noise.³⁹ Following Ref. 18 we also use this terminology for point-process noise. In this paper, we consider the unnormalized version of the KSE — the Zakai equation (ZE) — because it results in simpler equations throughout the derivation. When combined, the ZE and SDCKE represent the conditional (stochastic) evolution of the classical measurement device. The average evolution of the measurement device is contained within these equations, but is stochastic at this stage.

The evolution of the stochastic master equation, the SDCKE, and the ZE are combined to give the so-called¹⁸ joint stochastic equation. This equation governs the evolution of the measurement-device-plus-CQD supersystem. The next step in the derivation is to average over processes that a realistic observer would be unable to monitor. This removes the stochasticity that is due to unobservable microscopic processes (such as tunneling) and leaves the stochasticity associated with the measurement. After normalization, the resulting stochastic trajectory for the supersystem state is called¹⁸ a superoperator Kushner-Stratonovich equation (SKSE). The realistic quantum trajectory for the quantum system (CQD qubit in our case) is found by solving the SKSE, which must be done numerically. Thus, strictly speaking we derive an equation *whose solutions* are the realistic quantum trajectories for the qubit state.

A. Stochastic differential Chapman-Kolmogorov equation

A general stochastic differential equation (SDE), or Langevin equation, can be written in the Itô form as

$$dQ(t) = a(Q)dt + \sum_j \sqrt{D_j} dW_j(t) + \sum_k e_k dN_k(t), \quad (39)$$

where $Q \equiv Q(t)$ is a stochastic variable, $a(Q)$ is a general function of Q , $dW(t)$ and $dN(t)$ are stochastic increments and D_j and e_k are constants. The point increment $dN(t)$ was introduced in Sec. II B and the Wiener increment $dW(t)$ was introduced in Sec. III. For convenience in the steps that follow we will only use one term from each of the stochastic increment sums in Eq. (39). Generalization back to the multiple stochastic increments of Eq. (39) is simple.

The form of Eq. (39) is appropriate for situations where Q is known. Often it is not known in reality and we require an equation for the evolution of the probability distribution for Q , written $P(q)$. We now proceed to derive this equation.

If we assume for a moment that we know Q at time t (this is relaxed later), then $P(q)$ is a delta function: $P(q) = \delta(q - Q)$. The evolution of $P(q)$ follows

$$\begin{aligned} dP(q) &= d\delta(q - Q) \\ &= \delta(q - [Q + dQ]) - \delta(q - Q) \\ &= \delta\left(q - Q - a(Q)dt - \sqrt{D}dW - e dN\right) \\ &\quad - \delta(q - Q), \end{aligned} \quad (40)$$

where we have used Eq. (39) for dQ and time arguments have been omitted for simplicity. We shall only include time arguments when they aid the reader's understanding.

Converting the first term of Eq. (40) into a Taylor series about $q = Q$ yields an exponential. This exponential can be expanded to all orders and the expression simplified using the rules of Itô stochastic calculus: $dN^2 = dN$, $dW^2 = dt$ and all other products equal to zero.²⁷ This yields

$$\begin{aligned} d\delta(q - Q) &= \left\{ \frac{\partial}{\partial q} \left[-a(Q)dt - \sqrt{D}dW \right] \right. \\ &\quad \left. + \frac{D}{2} \frac{\partial^2}{\partial q^2} dt \right\} \delta(q - Q) \\ &\quad + dN [\delta(q - Q - e) - \delta(q - Q)]. \end{aligned} \quad (41)$$

Changing $a(Q)$ to $a(q)$ with the delta function and then averaging over the stochastic variable Q yields the Itô equation for the probability distribution $P(q) = E[\delta(q - Q)]$

$$\begin{aligned} dP^\mu(q) &= \left\{ \frac{\partial}{\partial q} \left[-a(q)dt - \sqrt{D}dW \right] + \frac{D}{2} \frac{\partial^2}{\partial q^2} dt \right\} P(q) \\ &\quad + dN [P(q - e) - P(q)], \end{aligned} \quad (42)$$

where the superscript μ denotes conditioning of this increment on the microscopic processes within the device; that is, the tunneling events (dN) and the Johnson noises (dW). This equation has been called²⁷ the stochastic differential Chapman-Kolmogorov equation (SDCKE). It includes a deterministic drift term (the first dt term), a stochastic drift term (the dW term), a diffusion term (the $\partial^2/\partial q^2$ term) and a stochastic jump term (the dN term). In the most general case this equation will have a sum of dW terms and a sum of dN terms.

B. Zakai equation

The SDCKE in the previous section can be used to describe the increment in $P(q)$ conditioned on the microscopic processes occurring within the measurement device. There is another stochastic increment to the probability distribution for Q . It represents evolution due to measurement of the current through the detector. The unnormalized expression for this stochastic evolution is called the Zakai equation (ZE) for the classical system (the measurement device). The normalized version is called the Kushner-Stratonovich equation (KSE).

The state of the measurement device is represented by the probability distribution $P(q)$ that was introduced in the previous section. The state of this classical system changes upon measurement and so $P(q)$ must be updated. The new probability distribution representing the conditioned state of the detector-circuit system, given a measurement result \mathcal{I} , is found using Bayesian analysis to be

$$\tilde{P}(q|\mathcal{I}) = \frac{P(\mathcal{I}|q)P(q)}{\Lambda(\mathcal{I})}, \quad (43)$$

where $\Lambda(\mathcal{I}) = P(\mathcal{I}|q = \beta/\alpha)$. Here the tilde denotes an unnormalized quantity and the value of $q = \beta/\alpha$ is chosen for convenience. $\Lambda(\mathcal{I})$ can be thought of as the *ostensible* probability distribution,¹⁶ as opposed to the actual probability distribution

$$\begin{aligned} P(\mathcal{I}) &= \int dq P(\mathcal{I}|q)P(q) \\ &= \Lambda(\mathcal{I}) \int dq \tilde{P}(q|\mathcal{I}), \end{aligned} \quad (44)$$

which would appear in the normalized expression $P(q|\mathcal{I})$. Here $P(q|\mathcal{I})$ is read 'the probability of q given \mathcal{I} '. The Zakai equation tells us how to update the probability distribution $P(q)$ when the measurement result \mathcal{I} is obtained. The quantity $P(\mathcal{I}|q)$ is the probability of obtaining the result \mathcal{I} given that the state is q . We will use the simpler notation $P_q(\mathcal{I}) \equiv P(\mathcal{I}|q)$, where the subscript denotes the result upon which the conditioning is performed.

The conditioning upon measurement depends on the form of the probability distributions involved in Eq. (43), which depend on the detector and circuit. From our expression for the measured current, Eq. (32), we expect

$P_q(\mathcal{I})$ to be a Gaussian distribution due to the Gaussian statistics of the Wiener process given in Eqs. (33). The mean and variance are given by the mean and variance of the current $\mathcal{I}(t)$. From Eq. (32) we find that $\mathcal{I}(t)$ has a variance of $\nu = (D_i + D_o)/dt$ and a mean of $m = -\alpha Q + \beta$ (assuming that we know Q for now).

Using the standard form of a Gaussian distribution with mean m and variance ν yields

$$P_q(\mathcal{I}) = \frac{1}{\sqrt{2\pi\nu}} \exp\left[-(\mathcal{I} - m)^2/2\nu\right]. \quad (45)$$

For $\Lambda(\mathcal{I})$ we use $q = \beta/\alpha$ in Eq. (45) which gives $m = 0$ so that

$$\Lambda(\mathcal{I}) = \frac{1}{\sqrt{2\pi\nu}} \exp\left[-\mathcal{I}^2/2\nu\right]. \quad (46)$$

We now calculate the conditioning on $P(q)$ due to measurement of the current using Bayesian analysis:

$$\begin{aligned} \tilde{P}_{\mathcal{I}}(q) &= \frac{P_q(\mathcal{I})P(q)}{\Lambda(\mathcal{I})} \\ &= \frac{\exp\left[-(\mathcal{I} - m)^2/2\nu\right]}{\exp\left[-\mathcal{I}^2/2\nu\right]} P(q) \\ &= \exp\left[-(m^2 - 2\mathcal{I}m)/2\nu\right] P(q), \end{aligned} \quad (47)$$

Expanding the exponential in Eq. (47) in a Taylor series to order dt and performing some simplifications yields the updated probability distribution after a measurement is made (the Zakai equation):

$$\tilde{P}_{\mathcal{I}}(q) = \left[1 + \mathcal{I}dt \frac{m}{D_{\Sigma}}\right] P(q), \quad (48)$$

where we have used $\nu \propto 1/dt$ and $\mathcal{I}^2/\nu^2 = 1/\nu$ which follows from the Itô rules²⁷ appropriate for the ostensible probability distribution $\Lambda(\mathcal{I})$. We have defined $D_{\Sigma} = D_i + D_o$ for convenience. We remind the reader that $m = -\alpha q + \beta$, while \mathcal{I} has the ostensible distribution in Eq. (46).

Both the SDCKE and ZE were derived independent of the detector and so are valid for all the detectors we consider.

C. Combining the stochastic increments

The next step is to combine the two probability increments $dP^{\mu}(q)$ and $d\tilde{P}_{\mathcal{I}}(q)$. This is done simply by applying Eq. (48) to the microscopically conditioned state $P^{\mu}(q)$ as follows

$$\tilde{P}(q) + d\tilde{P}_{\mathcal{I}}^{\mu}(q) = \left[1 + \mathcal{I}dt \frac{m}{D_{\Sigma}}\right] P^{\mu}(q), \quad (49)$$

where the microscopically conditioned state is given by the SDCKE (42).

D. Joint stochastic equation

The stochastic state of the joint classical-quantum system is found by forming the new conditional quantity

$$\tilde{G}_{\mathcal{I}}^{\mu}(q) = \tilde{P}_{\mathcal{I}}^{\mu}(q)G^{\mu}(t). \quad (50)$$

For the DC-SET A and QPC, ρ is used in place of G . The evolution of $\tilde{G}_{\mathcal{I}}^{\mu}(q)$ is described by the joint stochastic equation

$$\tilde{G}(q) + d\tilde{G}_{\mathcal{I}}^{\mu}(q) = [\tilde{P}(q) + d\tilde{P}_{\mathcal{I}}^{\mu}(q)] [G(t) + dG^{\mu}(t)]. \quad (51)$$

Here $dG^{\mu}(t)$ is the increment in the conditional state matrix of the quantum system (given by the Itô form of the ideal quantum trajectory) as derived in Sec. II.

Averaging over unobserved microscopic processes (μ) is the next step in the derivation of realistic quantum trajectory equations and yields an expression for $d\tilde{G}_{\mathcal{I}}(q)$. This process removes the stochasticity associated with the unobserved microscopic processes within the measurement device and leaves the stochasticity associated with the measurement. The resulting equation is called a superoperator Zakai equation (SZE) as we have obtained a quantum analogue of the ZE in that from measurement we are conditioning the state of a super-system that contains a quantum system. It is important to realize that after averaging over unobserved processes the super-system state $\tilde{G}(q) + d\tilde{G}_{\mathcal{I}}(q)$ will *not* factorize as in Eq. (51).

E. Normalization

Normalization of the SZE is the final step in deriving realistic quantum trajectory equations and yields the superoperator Kushner-Stratonovich equation (SKSE). The normalization is achieved as follows.

$$\begin{aligned} G(q) + dG_{\mathcal{I}}(q) &= \frac{\tilde{G}(q) + d\tilde{G}_{\mathcal{I}}(q)}{\int \text{Tr} [\tilde{G}_{\mathcal{I}}(q) + d\tilde{G}_{\mathcal{I}}(q)] dq} \\ &= \frac{\tilde{G}(q) + d\tilde{G}_{\mathcal{I}}(q)}{N(1 + dK)}, \end{aligned} \quad (52)$$

where $dK \equiv \frac{1}{N} \int \text{Tr} [d\tilde{G}_{\mathcal{I}}(q)] dq$ and $N \equiv \int \text{Tr} [\tilde{G}(q)] dq$. The binomial expansion can be used on Eq. (52) to yield

$$G(q) + dG_{\mathcal{I}}(q) = \frac{\tilde{G}(q) + d\tilde{G}_{\mathcal{I}}(q)}{N} [1 - dK + (dK)^2]. \quad (53)$$

After normalization the true expression for the observed current \mathcal{I} should be substituted into the SKSE. The true

probability distribution for \mathcal{I} can be found using Eq. (48) in Eq. (44) to yield

$$P(\mathcal{I}) = (2\pi\nu)^{-1/2} \exp \left[-(\mathcal{I} + \alpha \langle Q \rangle - \beta)^2 / 2\nu \right], \quad (54)$$

where $\langle Q \rangle = \int q P(q) dq$. Thus, the true expression for the actual observed current is

$$\mathcal{I} dt = (-\alpha \langle Q \rangle + \beta) dt + \sqrt{D_\Sigma} dW, \quad (55)$$

where dW is the observed white noise (a Wiener increment). Here the average is $\langle Q \rangle = \int q \text{Tr} [G(q)] dq$, since we are considering the output \mathcal{I} for the combined classical-quantum super-system.

The actual realistic quantum trajectory for the state of the qubit plus SET super-system state is obtained by solving the SKSE for $G(t)$, which must be performed numerically due to its stochastic nature.

V. EXAMPLE REALISTIC QUANTUM TRAJECTORY EQUATIONS

This section contains example realistic quantum trajectory equations for the DC-SET. The results are applicable to the DC-SET A and low transparency QPC upon making the substitutions $C_2 = 0$, $dN_2 = dN$ and using ρ in place of G , as discussed at the end of Sec. III. The theory presented in the preceding section is used.

A. Stochastic differential Chapman-Kolmogorov equation

Using the theory of Sec. IV A we obtain the following general SDCKE for the DC-SET:

$$\begin{aligned} dP^\mu(q) = dt & \left(-\frac{1}{F} \frac{\partial}{\partial q} m + \frac{D_i}{2F^2} \frac{\partial^2}{\partial q^2} \right) P(q) \\ & - \frac{\sqrt{D_i}}{F} \frac{\partial}{\partial q} dW_i P(q) \\ & + dN_1 [P(q - e_1) - P(q)] \\ & + dN_2 [P(q - e_2) - P(q)]. \end{aligned} \quad (56)$$

This is the increment in the probability distribution for the charge on the parasitic capacitor conditioned by the microscopic processes (μ) occurring within the realistic DC-SET.

B. Zakai equation

The ZE calculated in Sec. IV B was a general result for our measurement circuit and applies to all of the detectors we consider. We restate the result [Eq. (48)] here for completeness:

$$P(q) + d\tilde{P}_\mathcal{I}(q) = \left[1 + \mathcal{I} dt \frac{m}{D_\Sigma} \right] P(q). \quad (57)$$

This increment in the probability distribution for Q is conditioned by measurement of the realistic current \mathcal{I} .

C. Combining the stochastic increments

Our description of the stochastic conditional evolution of the classical measurement device is found by combining the increments $dP^\mu(q)$ and $d\tilde{P}_\mathcal{I}(q)$. The stochasticity of these two increments is related as the input noise dW_i plays a role in both. For this reason we must combine them into one increment using Eq. (49), rather than by simply adding them together. Remembering that we will eventually average over processes that cannot be observed by a realistic observer, the input noise needs to be separated into observed and unobserved parts. We express this as

$$dW_i = a \mathcal{I} dt + b dW' + c dt, \quad (58)$$

where

$$dW' \mathcal{I} dt = 0. \quad (59)$$

Here a , b and c are as yet undetermined expressions and dW' is unobserved, normalized white noise that is unrelated to the known output \mathcal{I} . When averages are taken, dW' will be averaged over and \mathcal{I} kept. The observed output [Eq. (32)] can be expressed as

$$\mathcal{I} dt = m dt + \sqrt{D_i} dW_i + \sqrt{D_o} dW_o. \quad (60)$$

Using Eqs. (58)–(60) gives the expression for dW' :

$$dW' = \frac{\sqrt{D_i} dW_o - \sqrt{D_o} dW_i}{\sqrt{D_\Sigma}}. \quad (61)$$

Using this in Eq. (58) and equating the left and right hand sides allows a , b and c to be determined. Substitution of a , b and c back into Eq. (58) yields

$$dW_i = \frac{\sqrt{D_i}}{D_\Sigma} \mathcal{I} dt - \sqrt{\frac{D_o}{D_\Sigma}} dW' - \frac{\sqrt{D_i}}{D_\Sigma} m dt. \quad (62)$$

Using this result and the SDCKE (56) in Eq. (49) gives

$$\begin{aligned} P(q) + d\tilde{P}_\mathcal{I}(q) = & \left\{ 1 + dt \left(-\frac{1}{F} \frac{\partial}{\partial q} m + \frac{D_i}{2F^2} \frac{\partial^2}{\partial q^2} \right) \right. \\ & + \left(m - \frac{D_i}{F} \frac{\partial}{\partial q} \right) \frac{\mathcal{I} dt}{D_\Sigma} \\ & + \left. \frac{1}{F} \sqrt{\frac{D_i D_o}{D_\Sigma}} \frac{\partial}{\partial q} dW' \right\} P(q) \\ & + dN_1 [P(q - e_1) - P(q)] \\ & + dN_2 [P(q - e_2) - P(q)]. \end{aligned} \quad (63)$$

Notice that the cross term between dW_i and $\mathcal{I} dt$ has canceled with the deterministic part of dW_i .

D. Joint stochastic equation

Following the approach presented in Sec. IV D, the joint stochastic equation¹⁸ describing the conditional

$$\begin{aligned}
d\tilde{G}_{\mathcal{I}}^{\mu}(q) = & \left\{ dt \left(-\frac{1}{F} \frac{\partial}{\partial q} m + \frac{D_i}{2F^2} \frac{\partial^2}{\partial q^2} \right) + \left(m - \frac{D_i}{F} \frac{\partial}{\partial q} \right) \frac{\mathcal{I} dt}{D_{\Sigma}} \right. \\
& + \frac{1}{F} \sqrt{\frac{D_i D_o}{D_{\Sigma}}} \frac{\partial}{\partial q} dW' + dt \left(\mathbb{E}[dN_1] + \mathbb{E}[dN_2] + \mathcal{L}_1 - \mathcal{S}_1 - \mathcal{S}_2 \right) \left. \right\} \tilde{G}(q) \\
& + dN_1 \left\{ \frac{\mathcal{S}_1 \tilde{G}(q - e_1)}{\mathbb{E}[dN_1]/dt} - \tilde{G}(q) \right\} + dN_2 \left\{ \frac{\mathcal{S}_2 \tilde{G}(q - e_2)}{\mathbb{E}[dN_2]/dt} - \tilde{G}(q) \right\}. \quad (64)
\end{aligned}$$

Averaging over the unobserved noise dW' and tunneling processes dN_1 and dN_2 yields the SZE

$$\begin{aligned}
d\tilde{G}_{\mathcal{I}}(q) = & \left\{ dt \left(\mathcal{L}_1 - \frac{1}{F} \frac{\partial}{\partial q} m + \frac{D_i}{2F^2} \frac{\partial^2}{\partial q^2} \right) \right. \\
& + \left(m - \frac{D_i}{F} \frac{\partial}{\partial q} \right) \frac{\mathcal{I} dt}{D_{\Sigma}} \left. \right\} \tilde{G}_{\mathcal{I}}(q) \\
& + dt \mathcal{S}_1 \left[\tilde{G}_{\mathcal{I}}(q - e_1) - \tilde{G}_{\mathcal{I}}(q) \right] \\
& + dt \mathcal{S}_2 \left[\tilde{G}_{\mathcal{I}}(q - e_2) - \tilde{G}_{\mathcal{I}}(q) \right], \quad (65)
\end{aligned}$$

evolution of the joint quantum-classical supersystem is

where we have now included the \mathcal{I} subscript on the right hand side because $\tilde{G}(q)$ is likely to have been conditioned by previous measurement results.

E. Normalization

Normalization of the SZE produces the SKSE and is performed via Eq. (53). We find that $dK = m\mathcal{I}dt/D_{\Sigma}$, which gives

$$\begin{aligned}
dG_{\mathcal{I}}(q) = & \left\{ dt \left(\mathcal{L}_1 - \frac{1}{F} \frac{\partial}{\partial q} m + \frac{D_i}{2F^2} \frac{\partial^2}{\partial q^2} \right) - \left[\alpha(q - \langle Q \rangle) + \frac{D_i}{F} \frac{\partial}{\partial q} \right] \frac{\mathcal{I} dt}{D_{\Sigma}} \right. \\
& + \frac{dt}{D_{\Sigma}} \left[(-\alpha \langle Q \rangle + \beta)^2 - (-\alpha \langle Q \rangle + \beta) \left(m - \frac{D_i}{F} \frac{\partial}{\partial q} \right) \right] \left. \right\} G_{\mathcal{I}}(q) \\
& + dt \mathcal{S}_1 [G_{\mathcal{I}}(q - e_1) - G_{\mathcal{I}}(q)] + dt \mathcal{S}_2 [G_{\mathcal{I}}(q - e_2) - G_{\mathcal{I}}(q)]. \quad (66)
\end{aligned}$$

We remind the reader that $\langle Q \rangle = \int q \text{Tr}[G(q)] dq$.

We now substitute in for the actual realistic detector output \mathcal{I} given by Eq. (55) to obtain the SKSE

$$\begin{aligned}
dG_{\mathcal{I}}(q) = & \left\{ dt \left[\frac{1}{F} \frac{\partial}{\partial q} (\alpha q - \beta) + \frac{D_i}{2F^2} \frac{\partial^2}{\partial q^2} \right] \right. \\
& - \frac{dW}{\sqrt{D_{\Sigma}}} \left[\alpha(q - \langle Q \rangle) + \frac{D_i}{F} \frac{\partial}{\partial q} \right] \left. \right\} G_{\mathcal{I}}(q) \\
& + dt \left\{ \mathcal{L}_1 G_{\mathcal{I}}(q) + \mathcal{S}_1 [G_{\mathcal{I}}(q - e_1) - G_{\mathcal{I}}(q)] \right. \\
& \left. + \mathcal{S}_2 [G_{\mathcal{I}}(q - e_2) - G_{\mathcal{I}}(q)] \right\}. \quad (67)
\end{aligned}$$

The first line of Eq. (67) describes the evolution of the classical measurement device. The second line consists of two terms. The first term describes information gain

about the detector (q) from its output Eq. (55). The second term describes back-action on the classical device due to the observed noise. The last two lines describe the evolution of the quantum system, some of which couples to the device.

The numerical solution of this equation would produce a trajectory for the state of the combined SET-CQD system. It is worth noting that the terms involving \mathcal{S}_1 and \mathcal{S}_2 represent average evolution due to electron tunneling events through the SET. They change the most likely value for the charge of the parasitic capacitor from Q to $Q - e_1$ ($Q - e_2$) when an electron tunnels onto (off) the SET island — effectively counting the average number of electrons passing through the SET. The approach of Ref. 40 involves a similar, but somewhat less realistic, technique in which they keep track of the exact number

of electrons that have passed through the SET.

For the SET it is simple to include other processes such as tunneling from drain to source and higher order processes such as co-tunneling, which tend to be important at higher temperatures.³⁵ We will leave the details of these procedures to a later paper to avoid distracting from the main results of this paper.

The classical nature of the SET island dot should also be considered.⁴⁹ This implies that there are no off-diagonal elements in the density matrix of the island dot and that

$$G = |0\rangle\langle 0| \otimes \rho^0 + |1\rangle\langle 1| \otimes \rho^1, \quad (68)$$

where $|0\rangle\langle 0|$ (not occupied) and $|1\rangle\langle 1|$ (occupied) are the possible states for the SET island dot. The states ρ^0 and ρ^1 are the state matrices for the qubit given these two conditions.

Using this, the SKSE for the DC-SET can be written as

$$\begin{aligned} d\rho_{\mathcal{I}}^0(q) = & dt \left\{ \left[\mathbf{L} - (r'_1 \mathcal{A}[\hat{n}] + r_1 \mathcal{A}[\hat{n}]) \right] \rho_{\mathcal{I}}^0(q) \right. \\ & \left. + \left[r'_2 \mathcal{J}[\hat{n}] + r_2 \mathcal{J}[1 - \hat{n}] \right] \rho_{\mathcal{I}}^1(q - e_2) \right\} \\ & - i \left[\hat{H}_{qb}, \rho_{\mathcal{I}}^0(q) \right] dt, \end{aligned} \quad (69a)$$

$$\begin{aligned} d\rho_{\mathcal{I}}^1(q) = & dt \left\{ \left[\mathbf{L} - (r'_2 \mathcal{A}[\hat{n}] + r_2 \mathcal{A}[\hat{n}]) \right] \rho_{\mathcal{I}}^1(q) \right. \\ & \left. + \left[r'_1 \mathcal{J}[\hat{n}] + r_1 \mathcal{J}[1 - \hat{n}] \right] \rho_{\mathcal{I}}^0(q - e_1) \right\} \\ & - i \left[\hat{H}_{qb} + \chi \hat{n}, \rho_{\mathcal{I}}^1(q) \right] dt, \end{aligned} \quad (69b)$$

which emphasizes the classical nature of the SET island dot. The classical operator \mathbf{L} represents the following evolution

$$\begin{aligned} \mathbf{L}\rho(q) = & \left\{ \frac{1}{F} \frac{\partial}{\partial q} (\alpha q - \beta) + \frac{D_i}{2F^2} \frac{\partial^2}{\partial q^2} \right. \\ & \left. - \frac{d\mathcal{W}(t)}{\sqrt{D_\Sigma}} \left[\alpha (q - \langle Q \rangle) + \frac{D_i}{F} \frac{\partial}{\partial q} \right] \right\} \rho(q). \end{aligned} \quad (70)$$

The normalized conditioned qubit state is found from

$$\rho_{\mathcal{I}}(t) = \sum_{m=0}^1 \int dq \rho_{\mathcal{I}}^m(q). \quad (71)$$

The realistic quantum trajectories are obtained by numerically solving the SKSEs and using Eq. (71). The results of this procedure will be presented in a future paper.

For completeness we also present the simpler SKSE for the other two detectors considered here — the DC-SET

A and QPC. The SKSE for the DC-SET A and QPC is

$$\begin{aligned} d\rho_{\mathcal{I}}(q) = & dt \left[\mathcal{L} + \frac{\partial}{\partial q} (\alpha q - \beta) + \frac{D_i}{2} \frac{\partial^2}{\partial q^2} \right] \rho_{\mathcal{I}}(q) \\ & - \frac{d\mathcal{W}}{\sqrt{D_\Sigma}} \left[\alpha (q - \langle Q \rangle) + D_i \frac{\partial}{\partial q} \right] \rho_{\mathcal{I}}(q) \\ & + dt \mathcal{S} [\rho_{\mathcal{I}}(q - e) - \rho_{\mathcal{I}}(q)], \end{aligned} \quad (72)$$

where the device-specific superoperators \mathcal{S} and \mathcal{L} are given in Sec. II B.

VI. DISCUSSION

A simple consistency check of our results (SKSEs) for the various detectors is to attempt to recover the relevant unconditional master equations. This can be done by averaging over the observed noise (by setting $d\mathcal{W} = 0$) and integrating the remaining terms in the SKSE over all q using the fact that *well-behaved* probability distributions (and their derivatives) vanish at $\pm\infty$. Using this technique it is easy to show that the SKSEs are consistent with the unconditional master equations.

A considerably more difficult task is to attempt recovery of the conditional master equations from the joint stochastic equations (the result before averaging over unobserved processes). In theory, this should be possible in the limit of a measurement circuit with a small response time given by $R_i C$ (large bandwidth $\alpha = (R_i C)^{-1}$) and low noises D_i and D_o . We explore this in the following two subsections.

A. Effective bandwidth of measurement device

The time taken to determine which CQD is occupied by the qubit electron is equal to the time required to ascertain the rate of tunneling through the detector. This task is made considerably more difficult by the white noise and finite bandwidth of the circuit containing the detector.

Consider the most general case of the DC-SET. Without the white noise the observer would see a spike in the current every time there was a tunneling event. In this case, because the two relevant rates of tunneling through the SET are greatly separated [see Eq. (2)], only a time equal to a small multiple of the average time between jumps for the SET in the conducting state would be needed to very accurately determine the SET state.

Depending on the relative sizes of the noise, the tunneling rates and the circuit response time, the white noise will obscure the spikes in the current so that the observer must rely on the *average* current to distinguish between the conducting and non-conducting SET states. The consequence of averaging out the white noise, by integrating the current \mathcal{I} over some time τ , is that if the qubit electron is tunneling on a time scale shorter than τ then the state of the quantum system cannot be followed.

We will now present an order of magnitude estimate of the effective bandwidth of the measurement device, which is defined as the frequency at which a signal power to noise power ratio of unity is obtained. Here we take the signal as being the current that flows off the detector when it is in the conducting state.

To find the noise and signal power we take the Fourier transform of Eqs. (32) and (38) in order to obtain the spectrum of the current \mathcal{I} . To simplify matters we consider tunneling through the detector as a single point process occurring at rate λ . This procedure is performed in Appendix B and gives results similar to those in Ref. 37. The signal power is

$$\lambda e^2 \frac{\alpha^2}{\alpha^2 + \omega^2 F^2} \quad (73)$$

and the noise power is

$$D_i \frac{\omega^2 F^2}{\alpha^2 + \omega^2 F^2} + D_o . \quad (74)$$

Upon equating the signal and noise powers, and at this frequency setting $\omega = \alpha_{\text{eff}}$, we have an effective bandwidth of

$$\alpha_{\text{eff}} = \frac{\alpha}{\sqrt{\mathbf{N}}} \sqrt{1 - \frac{D_o}{\lambda e^2}} \approx \frac{\alpha}{\sqrt{\mathbf{N}}} , \quad (75)$$

where the dimensionless noise parameter \mathbf{N} is defined according to

$$\mathbf{N} = \frac{(D_i + D_o) F^2}{\lambda e^2} . \quad (76)$$

The approximation of Eq. (75) holds in the limit where the noise power D_o is small compared to the signal power λe^2 (which is the regime that will lead to strong measurements of the qubit state). For an observer to be able to follow the evolution of the qubit reasonably well we must have $\alpha_{\text{eff}} > \Omega$.^{18,41}

The reader is reminded that we have ignored any capacitance in the cabling to the current amplifier, thus Eq. (75) should be used with caution. This comment also applies to the results of the next section.

B. Observation of SET tunneling events

If the SET measurement is being performed at a frequency for which the position of the qubit electron can be easily tracked, another more searching question may be asked: Can the tunneling events onto and off the SET island dot be detected?

The motivation for this question is the additional term $\chi \hat{b}^\dagger \hat{b} \otimes \hat{n}$ in the Hamiltonian \hat{H}_{SET} . Its effect can be seen by considering the case where the SET island dot is occupied, i.e. $\hat{b}^\dagger \hat{b} = 1$. In this case, the energy level in the nearby CQD is shifted up by χ which subsequently causes a shift in the CQD energy asymmetry. This is extra

back-action due to the measurement coupling between the SET and the nearby CQD that is absent in the case of a detector with a single tunnel junction. However, if the tunneling events in the SET can be tracked then this random phase shift is known and so does not affect the purity of the conditioned state. To answer the question above we compare the current that flows through the external circuit after a tunneling event to the current from the white noise. Similarly to distinguishing between the blockaded and conducting states of the SET, averaging of the white noise needs to be performed for the observer to have a chance of observing spikes. From Eqs. (32) and (38), the current in response to a single tunneling event through the left or right barrier that occurred a time t in the past (with $e_1 = e_2$) is

$$\frac{e\alpha}{2} \exp[-\alpha t] , \quad (77)$$

while that in response to the noise sources is [from Eq. (55)]

$$\sqrt{D_i + D_o} \frac{dW}{dt} . \quad (78)$$

Note that the input noise is being treated analogously to the output noise in this order of magnitude argument. That is, we are ignoring the fluctuating contribution to the capacitor charge from the input noise. This will be justified later.

If these currents are integrated for a time τ then we have a root-mean-square signal to noise ratio of

$$\frac{\frac{e}{2} (1 - \exp[-\alpha\tau])}{\sqrt{(D_i + D_o)\tau}} . \quad (79)$$

The optimal integration time, τ , will depend on the rate of tunneling through the SET, λ . It is not hard to show that the best signal to noise ratio for $\alpha \gg \lambda$ is of the order of α^{-1} , while if $\alpha \ll \lambda$ it is logical that it is approximately λ^{-1} . If we are integrating for a time α^{-1} , then frequencies of the order of α and below are important. At these frequencies the filtering of the input noise has a significant effect [from Eq. (74)], but the order of magnitude of its contribution will not be changed. If we are integrating for a time λ^{-1} , then frequencies of the order λ and below are relevant. Since $\lambda \gg \alpha$ for this integration time, from Eq. (74) we can see that the filtering is not likely to be important. Thus, ignoring the filtering of the input noise for both regimes is an acceptable order of magnitude approximation.

In the first regime ($\alpha \gg \lambda$) Eq. (79) becomes

$$\frac{e}{2} \sqrt{\frac{\alpha}{D_i + D_o}} , \quad (80)$$

implying that we are capable of observing the tunneling events if

$$\frac{e}{2} > \sqrt{\frac{D_i + D_o}{\alpha}} . \quad (81)$$

In the other regime ($\alpha \ll \lambda$) it follows that we can see tunneling if

$$\frac{e}{2} > \frac{\sqrt{\lambda(D_i + D_o)}}{\alpha}. \quad (82)$$

It is worth noting that this result (in the latter regime only) can be obtained using a different technique. In Eq. (67), the term which describes the effect of tunneling on the distribution for Q can be expanded to second order in the size of the jump. That is,

$$\lambda \left[G\left(q - \frac{e}{2}\right) - G(Q) \right] = \lambda \left[\frac{e}{2} \frac{\partial}{\partial q} + \frac{1}{2} \left(\frac{e}{2}\right)^2 \frac{\partial^2}{\partial q^2} \right] G(q), \quad (83)$$

where we have assumed that the size of the jump, $e/2$, is small compared to the standard deviation of the distribution of the parasitic capacitor charge. This may seem to be contradictory since we are trying to ascertain the regime for which the jumps are larger than the width of the distribution, but information can be obtained by allowing the width to approximate the jump size. Using the expansion in Eq. (83) we can find the variance of the distribution. Note that this involves ignoring the influence of the qubit, apart from the qubit placing the SET in a conducting state. In the limit $\alpha \ll \lambda$ we find that in order to see jumps Eq. (82) holds. It is perhaps not surprising that this technique does not give the same answer as Eq. (81) for $\alpha \gg \lambda$ since in this regime the expansion of Eq. (83) is unlikely to be valid.

C. DC-SET in comparison to the RF-SET

In experiments the capacitance of the cabling to the amplifier can be as large as 1nF. With a typical SET tunnel junction resistance of 100k Ω this will limit the operating frequency to the order of kilohertz.³² At these frequencies the charge sensitivity of SETs is limited by $1/f$ noise due to the motion of background charges. The intrinsic limit on the operation frequency of SETs, however, should be due to the RC time constant of the tunnel junctions themselves,³² which implies that frequencies of around gigahertz could be obtained. There have been various attempts, with some success, to circumnavigate the cabling capacitance. One obvious solution is to place the amplifier in close proximity to the SET, which is the type of circuit we are modeling when the cabling capacitance is being ignored. This was implemented in Ref. 42 and did improve the circuit performance somewhat. However, undesirable heating of the SET occurred.

It is unlikely that the problems involved with using a DC-SET circuit will be adequately resolved to the extent that the intrinsic limit of operation of the SET can be approached. Instead a different type of SET has become popular: the radio-frequency (RF) SET.^{32,43,44} In the RF-SET the read out of the charge state of the device is achieved by monitoring the damping of a high-frequency

resonant circuit to which the SET is connected. There are several advantages to this scheme. With the use of a low impedance, high frequency amplifier, the capacitance of the cabling is made unimportant.³² Since the amplifier can now be placed at a large distance from the SET it can also be optimized without worrying about heat dissipation. Also, $1/f$ noise is avoided because the read out is at such a high frequency. The operation frequency of the RF-SET has been demonstrated to be of the order of 100 megahertz, with sensitivities of above $10^{-5} e/\sqrt{\text{Hz}}$. These results represent a significant improvement upon the DC-SET.

Since the RF-SET will most likely prove to be the measuring device of choice for the read out of CQD qubits, it is an important task to derive and examine the relevant realistic quantum trajectories. This is a complex task, but major steps towards this end have been taken by the authors. The extra complexity is hinted at by the need for two circuit variables (the capacitor charge and the current through the inductor) rather than merely the capacitor voltage (as for the DC-SET). This work is continuing.

VII. CONCLUSION

A. Summary

We have presented a model for continuous measurement of a coupled quantum dot (CQD) charge qubit by a realistic DC-biased measurement device. We considered the dynamics of the measured qubit *conditioned* by measurement results for both the idealized measurement case and our new realistic measurement case. Our realistic measurement devices consist of ideal detectors embedded in an equivalent measurement circuit.

Our models for the conditional dynamics of the qubit due to ideal measurement by the DC-SET A and QPC were based on the quantum trajectory models of Wiseman, et al¹⁰ and Goan, et al,¹¹ respectively. Korotkov has derived equivalent conditional dynamics equations for the QPC (with notational differences) using a Bayesian formalism he developed.^{13,25,28,29,30}

For the case of ideal measurement we have presented stochastic master equations (quantum trajectories^{10,14,15,16}) that describe the time evolution of the measured qubit. For realistic measurement we applied a recently developed^{17,18} quantum trajectory theory presented for realistic photodetectors to realistic solid-state detectors. The solutions of the resulting stochastic equations are the quantum trajectories of the measured qubit state. These are termed “realistic quantum trajectories” and will be presented elsewhere.

Areas of application for the theory presented here include continuous quantum error correction (QEC), state preparation and feedback control for solid-state CQD charge qubits. Quantum trajectory theory can be used for the feedback control of open quantum systems,²³ but

has not previously incorporated the effects of a realistic measurement circuit. Therefore we expect our theory to play an important role in the development of realistic continuous QEC, state preparation and feedback control theories for CQD qubits and for open quantum systems in general.

B. Comparison to previous work

The conditional dynamics (also called “selective evolution”) of CQD systems measured by *ideal* detectors has been studied in Refs. 9,10,11,12,13, 25 and 28,29,30. However, the model of *realistic* measurement that we have presented in this paper is new. Korotkov has recently presented a phenomenological theory¹³ involving “non-ideal” detectors that is in the same spirit as ours (see Appendix A for a derivation of Korotkov’s result using the stochastic approach). However, he still assumed an infinite bandwidth detector and also assumed that the ideal detector could be described by diffusion rather than jumps. We believe that our *realistic* approach offers a more satisfying description of this measurement process because the effects of a realistic measurement circuit are included. These effects include thermal (white) noise and non-Markovian effects introduced by the finite bandwidths of realistic devices and circuits.

Finite detector temperature effects in the case of ideal measurement were not considered in our model. The effects of a non-zero detector temperature T_d have been considered previously^{11,25,45} and result in an approximately linear ($\coth [eV_d/2k_B T_d]$) increase in the ensemble decoherence rate and shot noise level with T_d for $eV_d < 2k_B T_d$, where V_d is the detector bias voltage. With a detector temperature of the order of mK,³¹ finite temperature effects could be expected to become important at bias voltages of $V_d < 0.3\mu V$. These voltages are several orders of magnitude below a sample bias voltage for maximum response of a SET detecting the charge state of a quantum dot,^{46,47} which suggests that the omission of finite detector temperature effects in the ideal detection scenario is reasonable.

To sum up, our realistic readout of CQD qubits is completely new. Previously this has only been considered for ideal measurement, with the exception of Korotkov’s phenomenological “non-ideal” model¹³ and Goan *et al*’s inefficiency¹¹ (which is perhaps better suited to photodetection in optics than to solid-state detectors¹³).

C. Future Work

There are many possibilities for future work in the theory of realistic quantum trajectories. As the field of mesoscopic electronics is progressing at such a tremendous rate it is likely that the choice of detector will quickly become outdated. In fact, the DC-SET has already been surpassed by the radio-frequency (RF) SET as the mea-

suring device of choice for the read out of the charge state of a mesoscopic qubit. This is one reason why we view the DC-SET work in this paper as preliminary work on SET measurements. The extension of realistic quantum trajectories to the RF-SET is a future aim.

Another reason for the necessity of further work on SETs is that the model we have presented for the DC-SET is somewhat simplified as the cabling to the current amplifier has been ignored. Apart from capacitive effects, a dissipative transmission line will also have dispersion. Thus, signals of different frequencies traveling down the line will move at different speeds and will be attenuated by different amounts.

These and other possibilities for work on the theory of realistic quantum trajectories will be pursued in the future.

Acknowledgments

Neil Oxtoby acknowledges Kate Cor for consistently entertaining and useful discussions.

APPENDIX A: DERIVATION OF KOROTKOV’S RESULT USING OUR APPROACH

In this appendix we derive an equivalent result to Korotkov’s phenomenological result for non-ideal detectors¹³ using a diffusive stochastic master equation approach and our method involving observed and unobserved noises.

We begin by defining a diffusive *linear* stochastic master equation¹⁶ for the state matrix of a measured two level system. The Itô stochastic master equation involving three classical, normalized white noise processes dW_0 (ideal detector output noise), dW_1 (extra output and backaction noise) and dW_3 (unobserved backaction noise) is

$$d\tilde{\rho} = dt\mathcal{L}\tilde{\rho} + dW_0\sqrt{\kappa_0}(\hat{\sigma}_z\tilde{\rho} + \tilde{\rho}\hat{\sigma}_z) + dW_1\sqrt{\kappa_1}\mathcal{H}[-i\hat{\sigma}_z]\tilde{\rho} + dW_3\sqrt{\kappa_3}\mathcal{H}[-i\hat{\sigma}_z]\tilde{\rho}, \quad (\text{A1})$$

where $\mathcal{L} = \mathcal{H}[-i\hat{H}] + (\kappa_0 + \kappa_1 + \kappa_3)\mathcal{D}[\hat{\sigma}_z]$ and $\hat{H} = \Omega\hat{\sigma}_x + \frac{1}{2}\varepsilon\hat{\sigma}_z$. The superoperator \mathcal{H} is defined by Eq. (9).

The three white noise processes dW_0 , dW_1 and dW_3 were chosen to correspond to Korotkov’s three unnormalized noise processes $\xi_0(t)$, $\xi_1(t)$ and $\xi_3(t)$. The white noise dW_0/dt represents the output of an ideal detector. Korotkov’s added output noise is known as dark noise,⁵⁰ which we model by setting the output of the realistic detector to be the current

$$\mathcal{I}(t)dt = \left(\sqrt{\phi_0}dW_0 + \sqrt{\phi_1}dW_1\right)/\sqrt{\phi_\Sigma}, \quad (\text{A2})$$

where ϕ_0 is the shot noise power (of the ideal detector output), ϕ_1 is the dark noise power and $\phi_\Sigma \equiv \phi_0 + \phi_1$. The normalization factor ensures that $\mathcal{I}(t)$ has a normalized Gaussian white noise distribution.

We now desire the quantum trajectory for the system state $\rho_{\mathcal{I}}$ conditioned on the realistic detector output in Eq. (A2) rather than on dW_0/dt . To proceed we rewrite dW_0 as

$$dW_0 = \left(\sqrt{\phi_0} \mathcal{I}(t) dt + \sqrt{\phi_1} dW' \right) / \sqrt{\phi_\Sigma}, \quad (\text{A3})$$

where $dW' = (\sqrt{\phi_1} dW_0 - \sqrt{\phi_0} dW_1) / \sqrt{\phi_\Sigma}$ is an unobserved normalized noise process that is independent of the observed output $\mathcal{I}(t)$. The extra output noise dW_1 can be expressed in terms of observed and unobserved quantities as

$$dW_1 = \left(\sqrt{\phi_1} \mathcal{I}(t) dt - \sqrt{\phi_0} dW' \right) / \sqrt{\phi_\Sigma}. \quad (\text{A4})$$

Substituting these into Eq. (A1) yields

$$\begin{aligned} d\tilde{\rho} = & dt \mathcal{L}\tilde{\rho} + \frac{\sqrt{\phi_0} \mathcal{I}(t) dt + \sqrt{\phi_1} dW'}{\sqrt{\phi_\Sigma}} \sqrt{\kappa_0} (\hat{\sigma}_z \tilde{\rho} + \tilde{\rho} \hat{\sigma}_z) \\ & + \frac{\sqrt{\phi_1} \mathcal{I}(t) dt - \sqrt{\phi_0} dW'}{\sqrt{\phi_\Sigma}} \sqrt{\kappa_1} \mathcal{H}[-i\hat{\sigma}_z] \tilde{\rho} \\ & + dW_3 \sqrt{\kappa_3} \mathcal{H}[-i\hat{\sigma}_z] \tilde{\rho}. \end{aligned} \quad (\text{A5})$$

The next step in our approach is to average over the unobserved noises dW' and dW_3 . The result is simply Eq. (A5) with the terms involving dW' and dW_3 absent.

Normalization of this result is performed in a similar manner as in Sec. IVE with the final result being the following non-linear SME:

$$\begin{aligned} d\rho = & dt \mathcal{L}\rho + \sqrt{\frac{\kappa_0 \phi_0}{\phi_\Sigma}} dt \left(\mathcal{I}(t) - 2 \langle \hat{\sigma}_z \rangle \sqrt{\frac{\kappa_0 \phi_0}{\phi_\Sigma}} \right) \mathcal{H}[\hat{\sigma}_z] \rho \\ & + dt \sqrt{\frac{\kappa_1 \phi_1}{\phi_\Sigma}} \left(\mathcal{I}(t) - 2 \langle \hat{\sigma}_z \rangle \sqrt{\frac{\kappa_0 \phi_0}{\phi_\Sigma}} \right) \mathcal{H}[-i\hat{\sigma}_z] \rho. \end{aligned} \quad (\text{A6})$$

Now we substitute in for the actual measured current

$$\mathcal{I}(t) dt = 2 \langle \hat{\sigma}_z \rangle \sqrt{\kappa_0 \phi_0 / \phi_\Sigma} dt + d\mathcal{W} \quad (\text{A7})$$

to obtain

$$\begin{aligned} d\rho = & dt \mathcal{L}\rho + \sqrt{\frac{\kappa_0 \phi_0}{\phi_\Sigma}} d\mathcal{W} \mathcal{H}[\hat{\sigma}_z] \rho \\ & + \sqrt{\frac{\kappa_1 \phi_1}{\phi_\Sigma}} d\mathcal{W} \mathcal{H}[-i\hat{\sigma}_z] \rho, \end{aligned} \quad (\text{A8})$$

which is equivalent to the non-ideal result of Korotkov in Ref. 13 with some notational differences.

APPENDIX B: SPECTRUM OF MEASURED CURRENT

In this appendix the spectrum of the current \mathcal{I} will be found. We will drastically simplify matters by considering tunneling through the SET as a single Poisson point process. That is, we put $e_1 dN_1(t) + e_2 dN_2(t) = (e/F) dN(t)$, with $E[dN(t)] = \lambda dt$. This derivation is based on the following equations

$$\dot{Q} = \frac{1}{F} \left(-\alpha Q + \beta + \sqrt{D_i} \frac{dW_i}{dt} + e \frac{dN}{dt} \right) \quad (\text{B1})$$

$$\mathcal{I} = -\alpha Q + \beta + \sqrt{D_i} \frac{dW_i}{dt} + \sqrt{D_o} \frac{dW_o}{dt}. \quad (\text{B2})$$

The spectrum can be calculated in a couple of ways. The first involves taking the Fourier transforms of Eqs. (B1) and (B2) and combining the results using the following current spectrum definition

$$S_{\mathcal{I}}(\omega) 2\pi \delta(\omega - \omega') = \langle \mathcal{I}(\omega) \mathcal{I}^*(\omega') \rangle. \quad (\text{B3})$$

The second method, used also in Ref. 37, is to find the steady-state current two-time autocorrelation function $G(\tau) = \langle \mathcal{I}(t) \mathcal{I}(t + \tau) \rangle_{\text{ss}} - \langle \mathcal{I} \rangle_{\text{ss}}^2$ and use Eq. (30). The first method results in the following current noise power spectrum (relative to the shot noise)

$$S_{\mathcal{I}}(\omega) = D_o + \frac{\omega^2 F^2}{\alpha^2 + \omega^2 F^2} D_i + \frac{\lambda e^2 \alpha^2}{\alpha^2 + \omega^2 F^2}. \quad (\text{B4})$$

The first two terms are the noise power and the final term is the signal power.

* Electronic address: Neil.Oxtoby@student.griffith.edu.au

† Electronic address: H.Wiseman@griffith.edu.au

¹ B. E. Kane, Nature (London) **393**, 133 (1998).

² D. Loss and D. P. DiVincenzo, Phys. Rev. A **57**, 120 (1998).

³ V. Privman, I. D. Vagner, and G. Kventsel, Phys. Lett. A **239**, 141 (1998).

⁴ A. Imamoglu, D. D. Awschalom, G. Burkard, D. P. DiVincenzo, D. Loss, M. Sherwin, and A. Small, Phys. Rev.

Lett. **83**, 4204 (1999).

⁵ R. Vrijen, E. Yablonovitch, K. Wang, H. W. Jiang, A. Balandin, V. Roychowdhury, T. Mor, and D. DiVincenzo, Phys. Rev. A **62**, 012306 (2000).

⁶ D. P. DiVincenzo, Science **270**, 255 (1995).

⁷ G. Burkard and D. Loss, Europhysics News **33** (2002).

⁸ L. M. K. Vandersypen, R. Hanson, L. H. Willems van Beveren, J. M. Elzerman, J. N. Griedanus, S. De Franceschi, and L. P. Kouwenhoven, in *Quantum Computing and*

- Quantum Bits in Mesoscopic Systems*, edited by A. J. Leggett, B. Ruggiero, and P. Silvestrini (Kluwer Academic/Plenum Publishers, New York, 2003).
- ⁹ S. A. Gurvitz, Phys. Rev. B **56**, 15215 (1997).
 - ¹⁰ H. M. Wiseman, D. W. Utami, H. B. Sun, G. J. Milburn, B. E. Kane, A. Dzurak, and R. G. Clark, Phys. Rev. B **63**, 235308 (2001).
 - ¹¹ H.-S. Goan, G. J. Milburn, H. M. Wiseman, and H. B. Sun, Phys. Rev. B **63**, 125326 (2001).
 - ¹² H.-S. Goan and G. J. Milburn, Phys. Rev. B **64**, 235307 (2001).
 - ¹³ A. N. Korotkov, Phys. Rev. B **67**, 235408 (2003).
 - ¹⁴ H. J. Carmichael, *An Open Systems Approach to Quantum Optics* (Springer, Berlin, 1993).
 - ¹⁵ H. M. Wiseman and G. J. Milburn, Phys. Rev. A **47**, 1652 (1993).
 - ¹⁶ H. M. Wiseman, Quantum Semiclass. Opt. **8**, 205 (1996).
 - ¹⁷ P. Warszawski, H. M. Wiseman, and H. Mabuchi, Phys. Rev. A **65**, 023802 (2002).
 - ¹⁸ P. Warszawski and H. M. Wiseman, J. Opt. B: Quantum Semiclass. Opt. **5**, 1 (2003).
 - ¹⁹ H. M. Wiseman and G. J. Milburn, Phys. Rev. Lett. **70**, 548 (1993).
 - ²⁰ H. M. Wiseman, Phys. Rev. Lett. **75**, 4587 (1995).
 - ²¹ M. A. Armen, J. K. Au, J. K. Stockton, A. C. Doherty, and H. Mabuchi, Phys. Rev. Lett. **89**, 133602 (2002).
 - ²² A. C. Doherty, S. Habib, K. Jacobs, H. Mabuchi, and S. M. Tan, Phys. Rev. A **62**, 012105 (2000).
 - ²³ H. M. Wiseman, S. Mancini, and J. Wang, Phys. Rev. A **66**, 013807 (2002).
 - ²⁴ W. P. Smith, J. E. Reiner, L. A. Orozco, S. Kuhr, and H. M. Wiseman, Phys. Rev. Lett. **89**, 133601 (2002).
 - ²⁵ A. N. Korotkov, Phys. Rev. B **63**, 115403 (2001).
 - ²⁶ R. Ruskov and A. N. Korotkov, Phys. Rev. B **66**, 041401 (2002).
 - ²⁷ C. W. Gardiner, *Handbook of Stochastic Methods for the Physical Sciences* (Springer, Berlin, 1985).
 - ²⁸ A. N. Korotkov, Phys. Rev. B **60**, 5737 (1999).
 - ²⁹ A. N. Korotkov, Phys. Rev. B **63**, 085312 (2001).
 - ³⁰ A. N. Korotkov, in *Quantum Noise in Mesoscopic Physics*, edited by Y. V. Nazarov (Kluwer Academic, Netherlands, 2003), pp. 205–228.
 - ³¹ H. Grabert and M. H. Devoret, eds., *Single Charge Tunneling: Coulomb Blockade Phenomena in Nanostructures* (Plenum Press, New York, 1992).
 - ³² R. J. Schoelkopf, P. Wahlgren, A. A. Kozhevnikov, P. Delsing, and D. E. Prober, Science **280**, 1238 (1998).
 - ³³ M.-S. Choi, F. Plastina, and R. Fazio, Phys. Rev. B **67**, 045105 (2003).
 - ³⁴ A. N. Korotkov, Phys. Rev. B **64**, 193407 (2001).
 - ³⁵ R. J. Schoelkopf, A. A. Clerk, S. M. Girvin, K. W. Lehnert, and M. H. Devoret, in *Noise and Information in Nanoelectronics, Sensors and Standards*, edited by L. B. Kish, F. Green, G. Iannaccone, and J. R. Vig (SPIE, 2003), vol. 5115, pp. 356–376.
 - ³⁶ G. J. Milburn and H. B. Sun, Contemporary Physics **39**, 1, 67 (1998).
 - ³⁷ N. P. Oxtoby, H.-B. Sun, and H. M. Wiseman, J. Phys.: Condens. Matter **15**, 8055 (2003).
 - ³⁸ G. E. P. Box and G. C. Tiao, *Bayesian Inference in Statistical Analysis* (Addison-Wesley, Sydney, 1973).
 - ³⁹ T. P. McGarty, *Stochastic Systems and State Estimation* (Wiley-Interscience, Sydney, 1973).
 - ⁴⁰ A. Shnirman and G. Schön, Phys. Rev. B **57**, 15400 (1998).
 - ⁴¹ P. Warszawski and H. M. Wiseman, J. Opt. B: Quantum Semiclass. Opt. **5**, 15 (2003).
 - ⁴² E. H. Visscher, J. Lindeman, S. M. Verbrugh, P. Hadley, J. E. Mooij, and W. van der Vleuten, Appl. Phys. Lett. **68**, 2014 (1996).
 - ⁴³ T. Fujisawa and Y. Hirayama, Appl. Phys. Lett. **77**, 543 (2000).
 - ⁴⁴ M. H. Devoret and R. J. Schoelkopf, Nature **406**, 1039 (2000).
 - ⁴⁵ R. Ruskov and A. N. Korotkov, Phys. Rev. B **67**, 075303 (2003).
 - ⁴⁶ D. Berman, N. B. Zhitenev, R. C. Ashoori, H. I. Smith, and M. R. Melloch, J. Vac. Sci. Technol. B **15**, 2844 (1997).
 - ⁴⁷ D. Berman, N. B. Zhitenev, R. C. Ashoori, and M. Shayegan, Phys. Rev. Lett. **82**, 161 (1999).
 - ⁴⁸ The engineering definition of the spectral density is a factor of two larger than Eq. (30) due to the addition of the negative and positive frequency components of the spectral density. See Ref. 35 for a detailed consideration of this.
 - ⁴⁹ This obviously applies only to the DC-SET.
 - ⁵⁰ This terminology is from quantum optics. Dark noise refers to electronic noise generated within a detector even when no field illuminates it, i.e. in the dark.